ADVANCES IN ATMOSPHERIC SCIENCES, VOL. 32, DECEMBER 2015, 1639–1646

Impact of UV-A Radiation on Erythemal UV and UV-index Estimation over Korea

Sang Seo PARK[1], Yun Gon LEE*[2], and Jung Hyun KIM[1]

[1]*Department of Atmospheric Sciences, Yonsei University, Seoul, Korea*
[2]*Department of Atmospheric Sciences, Chungnam National University, Daejeon, Korea*

(Received 17 October 2014; revised 26 May 2015; accepted 28 May 2015)

ABSTRACT

Because total UV (TUV) in the UV-A region is 100 times higher than in the UV-B region, UV-A is a considerable component when calculating erythemal UV (EUV) and UV-index. The ratio of EUV to TUV in the UV-A value [EUV(A)/TUV(A)] is investigated to convert the EUV(A) from TUV(A) for broadband observation. The representative value of EUV(A)/TUV(A), from the simulation study, is 6.9×10^{-4}, changing from 6.1×10^{-4} to 7.0×10^{-4} as aerosol optical depth, total ozone and solar zenith angle change. By adopting the observational data of EUV(B) and TUV(A) from UV-biometer measurements at Yonsei University [(37.57°N, 126.95°E), 84 m above sea level], the EUV irradiance increases to 15% of EUV(B) due to the consideration of EUV(A) from the data of TUV(A) observation. Compared to the total EUV observed from the Brewer spectrophotometer at the same site, the EUV(B) from the UV-biometer observes only 95% of total EUV, and its underestimation is caused by neglecting the effect of UV-A. However, the sum of EUV(B) and EUV(A) [EUV(A+B)] from two UV-biometers is 10% larger than the EUV from the Brewer spectrophotometer because of the spectral overlap effect in the range 320–340 nm. The correction factor for the overlap effect adjusts 8% of total EUV.

Key words: erythemal UV, total UV, UV-B, UV-biometer

Citation: Park, S. S., Y. G. Lee, and J. H. Kim, 2015: Impact of UV-A radiation on erythemal UV and UV-index estimation over Korea. *Adv. Atmos. Sci.*, **32**(12), 1639–1646, doi: 10.1007/s00376-015-4231-7.

1. Introduction

The solar radiation spectrum at the top of the atmosphere (TOA) mostly ranges from UV to visible. However, most of the UV radiation passing through the atmosphere is diminished through atmospheric extinction, especially absorption by stratospheric ozone. UV radiation is generally divided into UV-C (100–280 nm), UV-B (280–320 nm) and UV-A (320–400 nm). Among them, UV-C radiation does not reach the surface due to the oxygen and ozone absorption bands (e.g., Smith et al., 1992; Madronich et al., 1998). The two other spectral regions (i.e., UV-B and UV-A) do reach the surface, and cause biological damage such as erythema and skin aging in humans; however, spectrally, the extent of their influence differs. For this reason, erythemal UV (EUV) was introduced to quantify and monitor the effect of biological damage (e.g., Setlow, 1974; Caldwell et al., 1998; Madronich et al., 1998). EUV is calculated by multiplying the spectral UV irradiance by the spectral weighting function of the biological effect (i.e., erythema occurrence in skin). High weighting values are located in the UV-B wavelength ranges (e.g. McKinlay and Diffey, 1987).

Among the many ground-based measurements used to monitor the biological effective damage of UV radiation, two types of broadband and hyperspectral measurements have been most widely used. The UV-biometer is mostly used to measure the EUV over the UV-B wavelength range as the broadband type, and the Brewer spectrophotometer observes the spectral UV irradiance as the hyperspectral type. As EUV depends strongly on the spectral range of UV-B, broadband measurements consider the UV-B region only. For example, the UV-biometer 501 instrument mostly covers the spectral range of 280–320 nm (Solar Light Co., 1991). Considering the erythema weighting function up to 400 nm, the UV-A wavelength ranges are not considered in the EUV measurements by the UV-biometer. Despite the 100 times lower action spectrum values in UV-A, the spectral values of UV-A are 100 times higher than those in the UV-B region. Thus, the contribution of UV-A in estimating EUV from 280 nm to 400 nm needs to be analyzed. Furthermore, the wavelength range of this EUV is closely related to the definition of UV-index (WHO, 2002).

In Korea, the characteristics of UV radiation have been analyzed using the dataset from the UV-biometer and Brewer Spectrophotometer (e.g., Cho et al., 2001; Kim et al., 2011). Although these studies suggested the long-term trend and seasonal characteristics of EUV, the use of observational data

* Corresponding author: Yun Gon LEE
Email: yungonlee@gmail.com

including the UV-A wavelength range was insufficient. In particular, to estimate total UV (TUV), including UV-B and UV-A, the UV-biometer for UV-A can be used to supplement the limit of broadband observation with only the UV-B spectral range. Although many broadband observation sites have operated the two different broadband instruments simultaneously (i.e., the 501 UV-biometer and 501A UV-biometer), the UV-A information is not directly used for the EUV calculation over the range of 280–400 nm.

In this study, the contribution of UV-A in EUV is quantitatively analyzed by using simulation results and observation data. Furthermore, a possible method for accurately estimating EUV information from broadband-based observations is investigated. Also, in the process of considering the contribution of UV-A in EUV, correction factors to change the UV radiation are examined in various cases. Section 2 explains the method for EUV estimation from broadband TUV in the UV-A region. Section 3 presents the correction factors for conversion from TUV to EUV by the simulation in the UV-A region, and compares results between broadband and hyperspectral observations. Finally, the results are summarized, and their implications discussed, in section 4.

2. Methods

Because broadband observations record the data without spectral information, it is impossible for EUV to be directly estimated using the TUV data from broadband observation. Therefore, a correction factor calculation is essential to convert from TUV to EUV in the UV-A region. To restore the spectral information in the UV-A region, the radiative transfer model UVSPEC is used (Mayer and Kylling, 2005). The UV irradiance is calculated from 250 to 400 nm, with a spectral resolution of 0.1 nm, by considering the total ozone and aerosol information.

Figure 1 shows the input values for solar zenith angle (SZA), total ozone, aerosol optical depth (AOD) and single scattering albedo (SSA). The values of SZA and total ozone are the monthly representative data for Seoul. The monthly means of total ozone range from 288 to 374 Dobson Unit (DU). The AOD and SSA at 500 nm represent the monthly mean for 1 year's measurements from December 2006 to November 2007 in Seoul, as noted by Koo et al. (2007). The AOD ranges from 0.28 to 1.13 and the SSA from 0.90 to 0.94. Because the data quality of the aerosol measurements is relatively low in March (Koo et al., 2007), the AOD and SSA in March is replaced by the April data in the simulation by the radiative transfer model.

To adopt and validate the effect of UV-A in EUV, it is essential that the spectral and broadband UV measurements are both observed at one site. The site at Yonsei University, which is located in the northwest of Seoul [(37.57°N, 126.95°E), 84 m above sea level], has simultaneously operated two UV-biometers (a 501 UV-biometer and 501A UV-biometer), and a Brewer spectrophotometer. In addition, the UV-biometers and Brewer spectrophotometer have been

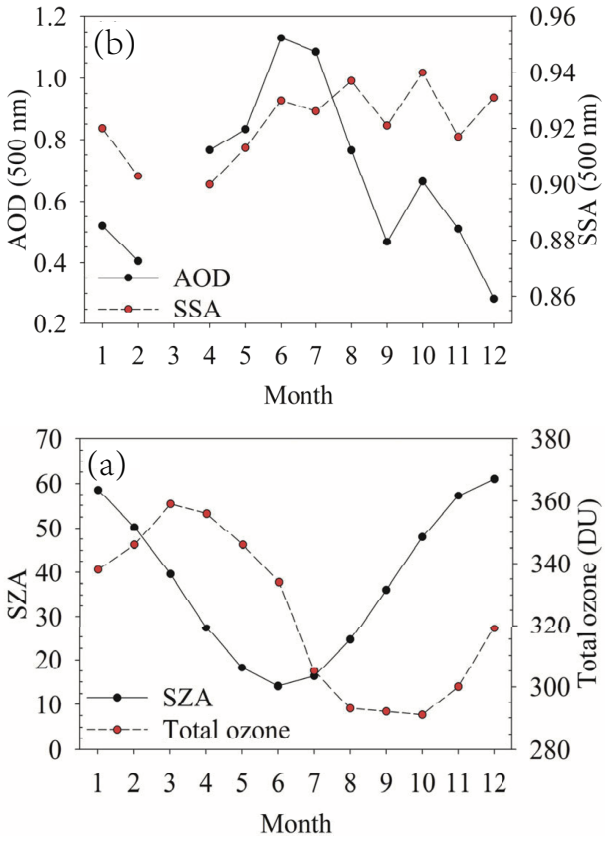

Fig. 1. (a) Input values of the UVSPEC simulation for monthly SZA and total ozone, and (b) aerosol optical properties.

managed, respectively, since 1995 and 1998. Specifically, this site has used the two different types of UV-biometer: the 501 UV-biometer, which measures the broadband EUV(B) (280–320 nm), by multiplying UV-B irradiance (280–320 nm) by the erythemal weighting function; and, similar to the 501 UV-biometer, the 501A UV-biometer, which measures the broadband UV(A) [320–400 nm, i.e., TUV(A) in this study], by integrating UV-A irradiance from 320 nm to 400 nm without the erythemal weighting function. Solar Light Co (2006). provides the detailed spectral response function of UV-biometer for erythema in the overall UV spectral range of 250–400 nm. We use the radiative transfer model to estimate the factor for converting from TUV(A) into EUV(A), and we actually apply the spectral response function over the spectral range of 320–400 nm in this process. WMO (2011) recommended that the uncertainty of broadband instruments for UV measurement is less than 5%, and thus the accuracy of the UV-biometer 501 satisfies the WMO guidelines.

The spectral UV irradiance from 286.5 to 363.0 nm is observed by the Brewer spectrophotometer (MK-IV, Instrument number: 148) with a spectral bandwidth of 0.6 nm and a spectral sampling of 0.5 nm. After observing the spectral range in UV, the Brewer spectrophotometer expresses the UV irradiance for the TUV and EUV as a selection. Therefore, the spectral UV data from the Brewer spectrophotometer can be used as a reference to compare with the broadband data from

the UV-biometers. In this study, the UV data observed by the UV-biometers and the Brewer spectrophotometer in the year 2007 are used, because the detailed aerosol optical properties were continuously recorded at the Seoul site in this year with confident accuracy.

3. Results

3.1. *Impact of UV-A on the EUV calculation*

Figure 2 shows the spectral irradiance of the TUV and EUV from the UVSPEC simulation in representative cases in January and July. The vertical line in the middle is the spectral border line between UV-A and UV-B. Because of the characteristics of the spectral erythema weighting function, most of the EUV irradiance is estimated in the UV-B region, and the maximum value is estimated within the spectral range of 300–310 nm. However, the EUV irradiance in the UV-A region is also estimated to carry significant values. For example, the irradiance is estimated to be 0.3–0.8 mW m^{-2} nm^{-1} at 330 nm, which is about 10% of the irradiance at 315 nm. This significant value is caused by the large intensities of TUV in the UV-A region, which is estimated to be larger than 100 mW m^{-2} nm^{-1}. However, because the effect of UV-A on EUV is spectrally varied, it is impossible to directly estimate the impact of UV-A on EUV from broadband observation.

The impact of UV-A on the EUV estimation is also shown in the broadband observation. Figure. 3a shows the time series of EUV from the 501 UV-biometer compared to those from the UVSPEC simulation. In selecting the input parameters of the UVSPEC calculations, the daily total ozone amounts measured from a Dobson spectrophotometer (instrument number: 124, WMO/Global Atmosphere Watch (GAW) station No. 252) are used. Thus, the UVSEPC simulations shown in Fig. 3 indicate the standards of UV-index under clear-sky conditions; the AOD at 550 nm of 0.2 and SSA

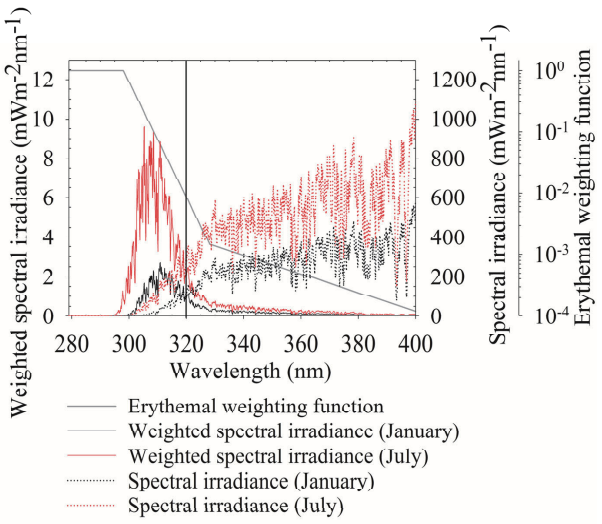

Fig. 2. Spectral irradiance of EUV and TUV from the UVSPEC simulation.

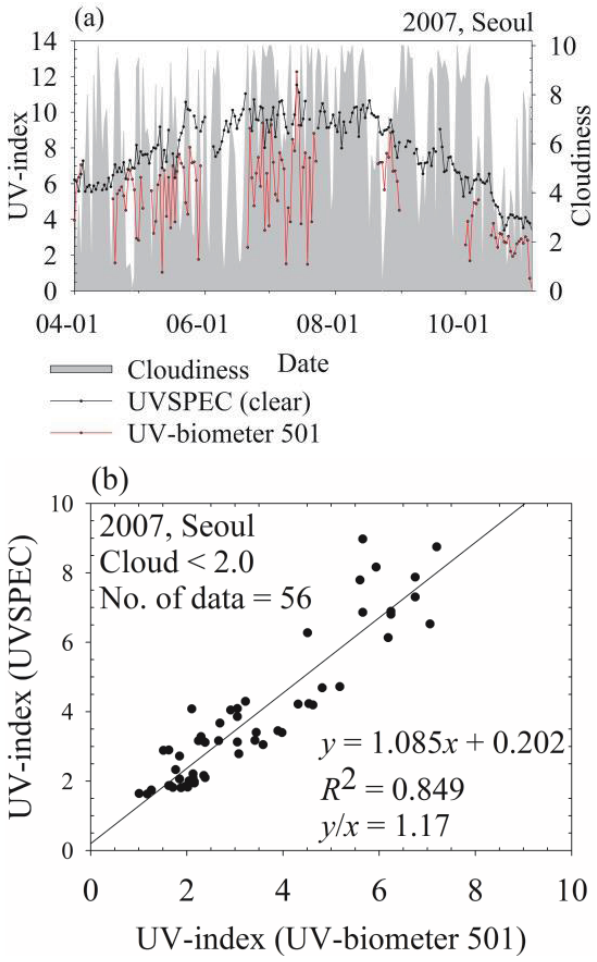

Fig. 3. (a) Time series of the UV-index estimated from the UVSPEC simulation and UV-biometer 501, and (b) its scatter plot in clear-sky conditions.

of 0.98 for the background aerosol condition, and cloud-free conditions are assumed. As observational data are contaminated by cloud and hazardous aerosol events, the overall observational data are lower than the simulation. Additionally, the limit of spectral coverage in broadband observation may be a factor influencing the underestimation of the observation. From the comparison result under the condition below daily cloudiness of 2.0, as shown in Fig. 3b, the slope between the UVSPEC simulation and observation from the 501 UV-biometer is 1.085, with a correlation coefficient of 0.849.

Table 1 shows the monthly EUV irradiance and UV-index from the UVSPEC simulation. Also shown is the ratio of the sum of EUV(B) and EUV(A) [EUV(A+B)] to the EUV(B) [EUV(A+B)/EUV(B)] from the simulation results. To define the irradiance of EUV(A) and EUV(B), the integrated spectral range is defined from 320 to 400 nm, and from 280 to 320 nm for EUV(A) and EUV(B), respectively. Compared to the EUV(B) and EUV(A+B), the difference of UV-index between EUV(A+B) and EUV(B) is estimated to be 0.6 to 1.2, which means that the UV-index has been underestimated due to lack of consideration of UV-A, and this effect can be significant to the broadband observation.

Table 1. Monthly EUV irradiance and the ratio of EUV(A+B) to EUV(B) from the UVSPEC simulation.

Month	EUV irradiance (mWm^{-2})(UV-index)		
	EUV(A+B)	EUV(B)	(A+B)/B
Jan	42.9 (1.71)	27.9 (1.12)	1.69
Feb	69.1 (2.76)	48.4 (1.94)	1.52
Mar	87.7 (3.51)	64.2 (2.57)	1.43
Apr	128.1 (5.12)	99.5 (3.98)	1.31
May	164.2 (6.57)	132.7 (5.31)	1.25
Jun	162.4 (6.50)	132.1 (5.28)	1.24
Jul	175.7 (7.03)	145.8 (5.83)	1.20
Aug	185.9 (7.44)	154.5 (6.18)	1.20
Sep	147.0 (5.88)	118.6 (4.74)	1.25
Oct	84.1 (3.36)	63.9 (2.56)	1.36
Nov	48.0 (1.92)	32.9 (1.32)	1.57
Dec	39.5 (1.58)	24.5 (0.98)	1.81

*The monthly representative values in April of AOD and SSA are used.

Table 2. Monthly TUV(A), EUV(A) and EUV(A)/TUV(A), as simulated by UVSPEC.

Month	Irradiance (mWm^{-2})		
	TUV(A) ($W\ m^{-2}$)	EUV(A) ($mW\ m^{-2}$)	EUV/TUV ($\times 10^{-4}$)
Jan	22.62	14.98	6.6
Feb	30.77	20.64	6.7
Mar	34.83	23.48	6.7
Apr	41.87	28.6	6.8
May	45.7	31.52	6.9
Jun	43.91	30.27	6.9
Jul	43.21	29.87	6.9
Aug	45.24	31.47	7.0
Sep	41.15	28.43	6.9
Oct	29.71	20.21	6.8
Nov	22.73	15.16	6.7
Dec	22.84	15.02	6.6

The EUV(A+B)/EUV(B) is estimated to be in the range from 1.2 to 1.8, and the ratio is strongly dependent on the representative monthly conditions. The annual variation of the ratio is caused by the SZA, aerosol, and total ozone amounts, which affect the scattering and absorption properties of UV radiation. The SZA causes change in the optical path length, and makes the optical depth change at the slant path. Furthermore, the extinctions for aerosol and total ozone are normally stronger in the UV-B region than in the UV-A region due to the spectrally strong dependence of the extinction -such as Rayleigh scattering and absorption. Therefore, the characteristics of extinction due to aerosol and total ozone also lead to the annual variation of the EUV(A+B)/EUV(B). Therefore, linear conversion from EUV(B) to EUV(A+B) is insufficient to determine the total amount of EUV irradiance.

To identify the EUV(A+B) from the broadband observation, the ratio of EUV(A)/TUV(A) is introduced in this study, defined as follows:

$$\mathrm{EUV(A)/TUV(A)} = \int_{\lambda_1}^{\lambda_2} W(\lambda) I(\lambda) d\lambda \Big/ \int_{\lambda_1}^{\lambda_2} I(\lambda) d\lambda \ ,$$

where $W(\lambda)$ is the erythema weighting function, as normalized by the weighting at 298 nm (McKinlay and Diffey, 1987), and $I(\lambda)$ is the spectral irradiance at wavelength λ. To calculate EUV(A)/TUV(A), the spectral irradiance data from the simulation is necessary. Table 2 shows the estimated TUV(A), EUV(A) and the EUV(A)/TUV(A) in the monthly representative cases. Because the erythema weighting function in the UV-A region is smaller than 8.0×10^{-3}, the order of EUV is 1000 times smaller than that of TUV. The value of EUV(A)/TUV(A) ranges from 6.6×10^{-4} to 7.0×10^{-4}, and EUV(A)/TUV(A) is larger in summer than in winter. For the period from April to September when EUV is strong, EUV(A)/TUV(A) is estimated to be 6.8×10^{-4} to 7.0×10^{-4}, and the representative value is estimated to be 6.9×10^{-4}.

Figure 4 shows the EUV(A)/TUV(A) in clear cases as a function of SZA, total ozone, and the AOD at 550 nm. For the calculation shown in the figure, the following conditions are assumed: SSA = 0.90; day of year = 75; altitude = 84 m (the altitude of the Yonsei University site). Furthermore, reference conditions of SZA = 30°, total ozone = 340 DU, and AOD at 550 nm = 0.4, are assumed. As shown in Fig. 4a, the EUV(A)/TUV(A) is estimated to be 6.1×10^{-4} to 7.0×10^{-4}, and the ratio rapidly decreases due to the large SZA. The extinction of spectral irradiance is relatively high at short wavelengths due to the spectral characteristics of Rayleigh scattering and absorption by ozone. For this reason, the decreased intensity of spectral irradiance is large at short wavelengths as the path length increases. Furthermore, the erythema weighting function has a large portion in short wavelengths, especially those shorter than 328 nm. A relatively large portion of the weighting function and strong extinction at short wavelengths affects the decrease in EUV(A)/TUV(A) as the SZA increases. Therefore, EUV(A)/TUV(A) is relatively sensitive to the change at short wavelengths, and optical path length, which affects the air-mass factor, the secant function of the SZA.

As suggested by the results shown in Fig. 4b, EUV(A)/TUV(A) is significantly influenced by the total ozone value. Although the strong absorption by ozone is mostly found in the UV-B region, the absorption band of ozone in the UV-A region below 350 nm is also important, referred to as the Huggins band (e.g., Inn and Tanaka, 1953; Griggs, 1968; Le Quéré and Leforestier, 1992). Based on Molina and Molina (1986), the absorption cross section of ozone is estimated to be 0.377×10^{-20} cm^2 $molecule^{-1}$ at 330.0 nm and 0.167×10^{-20} cm^2 $molecule^{-1}$ at 340.0 nm, if the temperature is assumed to be 263 K. Therefore, the irradiance in the UV-A region is partially affected by the total ozone amount, which causes the decrease of EUV(A)/TUV(A) as the total ozone amount increases. From the simulation in the reference case, the decreasing rate of EUV(A)/TUV(A) in the total ozone is estimated to be -1.0×10^{-5} $(100\ DU)^{-1}$. For example, the maximum and minimum value of total ozone at Seoul was 499 and 225 DU from 1985 to 2009, respectively (Park

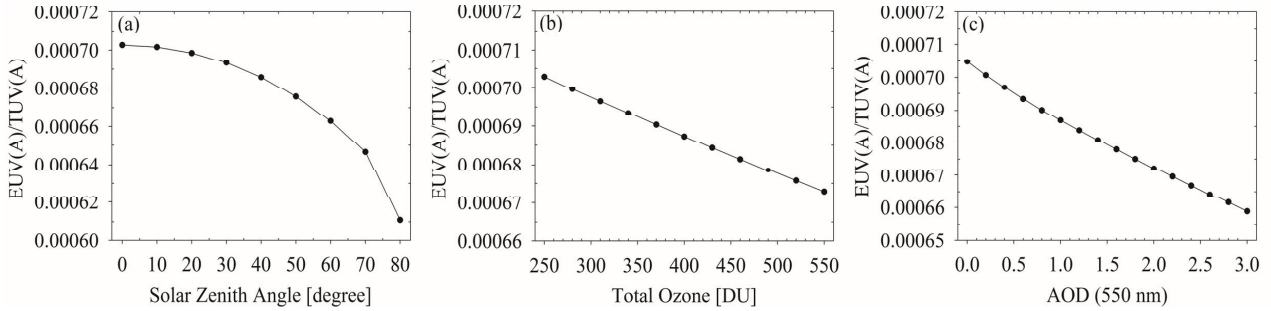

Fig. 4. Simulated EUV(A)/TUV(A) in clear cases as a function of (a) SZA, (b) total ozone, and (c) AOD at 550 nm.

et al., 2011). Therefore, the variance of EUV(A)/TUV(A) is 2.7×10^{-5}, which is equal to 3.9% of the relative variance. Figure. 4c shows the change of EUV(A)/TUV(A) due to the AOD change at 550 nm. Similar to the results shown in Fig. 4b, the EUV(A)/TUV(A) decreases with increasing AOD, and the slope of EUV(A)/TUV(A) with respect to AOD is -1.5×10^{-5}. From observation at Seoul, the Angström exponent of aerosol is estimated to be in the range from 0.905 to 1.193 (Koo, 2008). For this reason, the spectral change of AOD normally decreases as the wavelength increases, producing the decrease of EUV(A)/TUV(A). Kim et al. (2007) revealed that the monthly mean of AOD over East Asia to be lower than 2.0. When this value is considered as the maximum value, the relative variance of EUV(A)/TUV(A) due to the AOD is estimated to be about 4.4%.

3.2. *Long-term validation (Year 2007)*

To calculate the EUV(A+B) from the broadband observation, the EUV(A)/TUV(A) is adopted to convert from the observed TUV(A) to the EUV(A). Figure 5 shows a scatter plot of the EUV irradiance between the Brewer spectrophotometer and the UV-biometers. To adjust the observation time, the time difference between the Brewer spectrophotometer and the UV-biometers is established to be less than 30 seconds for the comparison. Furthermore, the EUV data from the Brewer spectrophotometer that are larger than 10 mW m^{-2} are used for the validation, to neglect the effect of large-scale clouds (number of data = 560). The EUV(A)/TUV(A) value uses the fixed value of 6.9×10^{-4}, as described above. From Fig. 5a, the EUV(B) from the UV-biometer 501 is partially underestimated, as compared to the EUV from the Brewer spectrophotometer. Although the correlation coefficient (R^2) is 0.820, which is a statistically significant value, the slope is estimated to be 0.951. This statistical result means that the observation of the UV-biometer 501 in the UV-B region only explains 95.1% of the total irradiance of EUV from the Brewer spectrophotometer. To adopt the EUV(A) value by using the TUV data from the UV-biometer 501A in the UV-A region, the slope is calculated to be 1.103 and the R^2 is 0.818, as shown in Fig. 5b. Compared to Fig. 5a, the R^2 value is almost the same but the slope is significantly improved; the intensity of enhancement is about 0.152. From this result, the EUV in the UV-A region is calculated to take about 15% of the EUV irradiance, which is comparable to previous findings (van Geffen et al., 2004).

To consider the different conditions for aerosol and total ozone amount, a look-up table (LUT) for EUV(A)/TUV(A), which adopts the observed TUV(A) data, is developed. The LUT considers the change of SZA, AOD, and total ozone amount. To cover most of the observed conditions, the EUV(A)/TUV(A) value is estimated in the LUT for cases in which the SZA ranges from 0.0° to 80.0°, with a 10.0° degree interval; the AOD ranges from 0.0 to 3.0, with an interval of 0.2; and the total ozone ranges from 250 to 550 DU, with a 30 DU interval. From the LUT simulation, the EUV(A)/TUV(A) is calculated to be $6.60 \times 10^{-4} \pm 0.35 \times 10^{-4}$ (1-σ level).

Figure 6 shows a similar result as Fig. 5, but the ratio of EUV(A)/TUV(A) is used from the LUT simulation, as changed by the conditions of AOD and total ozone. The AOD and total ozone values are daily averaged data from the Brewer spectrophotometer. Because the reference wavelength of the AOD measured by the Brewer spectrophotometer is 320.1 nm, the Angström exponent is assumed to be 1.0, which is the mean value (340–1020 nm) in 2007 at Seoul (Koo, 2008), to estimate the AOD at 550 nm. From the scatter plot, the slope and R^2 value are estimated to be 1.107 and 0.819, respectively. Compared to Fig. 5b, the slope and R^2 value show insignificant differences. The difference of the statistical result between Fig. 5b and Fig. 6 is related to the variation of EUV(A)/TUV(A) as a consideration of total ozone and aerosol, and the proportion of EUV(A) to total EUV. The proportion of EUV(A) to total EUV is about 15% from the previous result, and the EUV(A) difference between the fixed and LUT method for EUV(A)/TUV(A) is $2.1\% \pm 2.3\%$. Therefore, the effect of AOD and total ozone is insignificant during the comparison period.

From Figs. 5b and 6, the EUV(A+B) from the UV-biometers is partially overestimated compared to that from the Brewer spectrophotometer. The reason for the overestimation is caused by the sensitivity of UV-A for the 501 UV-biometer in the UV-B observation. Kudish et al. (2005) reported that the normalized spectral response is ∼0.001 at 330 nm, which is about 10% of the sensitivity at 320 nm. Furthermore, Singh et al. (2005) showed that the UV-B biometer actually measures the spectral band of 280–340 nm, by using the broadband filter characteristics. Although the absolute value of the spectral response is small, this sensitiv-

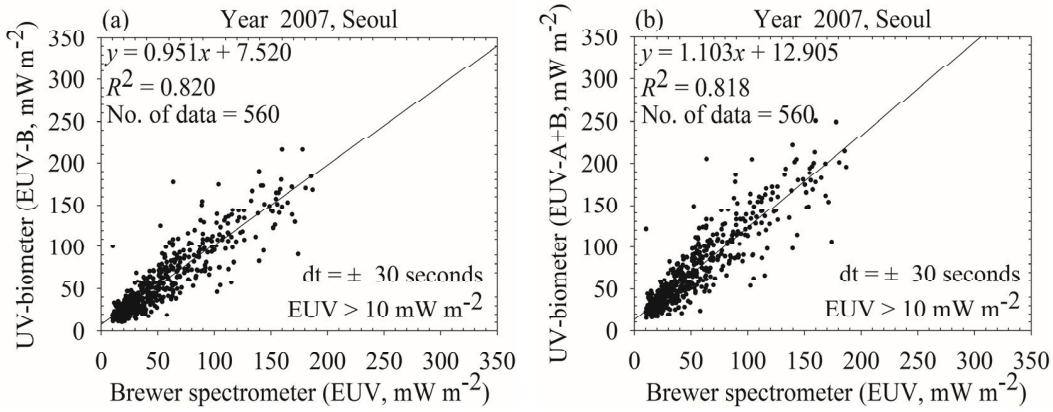

Fig. 5. (a) Comparison of EUV irradiance between the Brewer spectrometer and the UV-biometers in the UV-B region, and (b) EUV(A+B) as estimated by the EUV(A) from the TUV(A) converted by the fixed EUV(A)/TUV(A). "dt" means time difference of observation between two instruments.

ity significantly affects the EUV calculation because the erythema weighting function is also small at this wavelength. For this reason, the effect of spectral overlap has to be subtracted for accurately estimating the EUV irradiance from the broadband observations. To correct the spectral overlap between 320 and 340 nm, the ratio of the spectrally integrated EUV (280–320 nm) to EUV (280–340 nm) is calculated as a function of SZA, AOD, and total ozone. Thus, an LUT of the ratio with the same dimension, identical to the LUT of EUV(A)/TUV(A), is considered. In addition, another LUT for EUV, spectrally integrated from 363 to 400 nm, is developed to supplement the spectral coverage of the Brewer spectrophotometer. Because of the limited spectral coverage of the Brewer spectrophotometer up to 363 nm, it potentially affects the comparison of spectral EUV integration between the UV-biometers and the Brewer spectrophotometer.

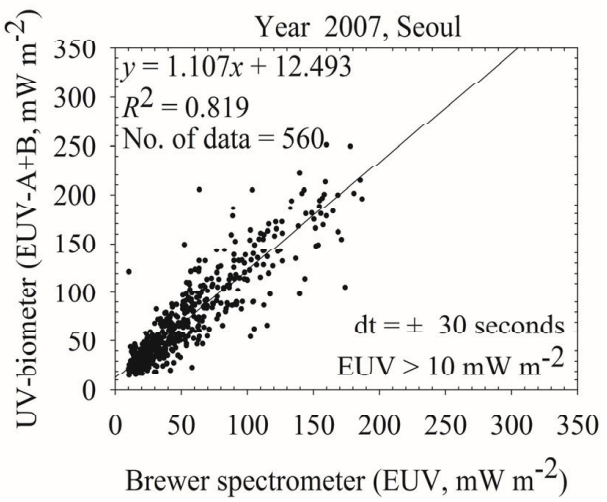

Fig. 6. Comparison of EUV irradiance between the Brewer spectrometer and the EUV(A+B) from the UV-biometers by using the LUT of EUV(A)/TUV(A). "dt" means time difference of observation between two instruments.

Figure 7 shows a scatter plot between the EUV from the Brewer spectrophotometer and the EUV(A+B) from the two different UV-biometers, after correcting the spectral coverage of the instruments using the two methods. Firstly, Fig. 7a compares the two EUVs; the EUV(B)+EUV(A) from the two UV-biometers minus the overlap of 320–340 nm and EUV(B + partial A) from the Brewer UV scans are examined using each LUT of the EUV(320/340) and EUV(A)/TUV(A) ratios. A close look at the statistics reveals a slope of 1.022 with standard deviation of 0.019 and the R^2 of 0.835. Compared to the previous results in Figs. 5b and 6, the slope between two values is decreased and the correlation coefficient is slightly better. Thus, the former overestimation of the EUV(A+B) calculated from the UV-biometers is to some extent corrected by removing the overlap effect of EUV(320/340). Secondly, Fig. 7b compares the Brewer UV scan extended from 363 nm to 400 nm. This result indicates a slope of 0.992 with standard deviation of 0.019, and an R^2 similar to that in Fig. 7a. While there are no significant differences for the two comparisons in the slope and R^2 values, the slope is more precisely fitted on a 1:1 line (i.e., slope of 1.0) by considering the expansion of the Brewer UV scan.

From the statistical analysis, the broadband observation of the EUV(B) accounts for about 85% of total EUV from the Brewer spectrophotometer, and its underestimation is caused by neglecting the contribution of UV-A. By adding the broadband UV-A data, the total EUV irradiance from broadband observation is increased by about 15%. It can be further suggested that the enhancement of the EUV value by considering UV-A is larger than the inherent uncertainty of the instrument. Although the effect of spectral overlap within 320–340 nm causes overestimation by 10%, the correction factor of the EUV(320/340) can reduce the overlap effect to about 8% of total EUV, and the spectral limitation of the Brewer spectrophotometer explains the remainder of the overestimation. Through several correction methods, the correlation coefficient is increased from 0.818 to 0.836. The calibration of the instrument is one of main effects of the discrepancies be-

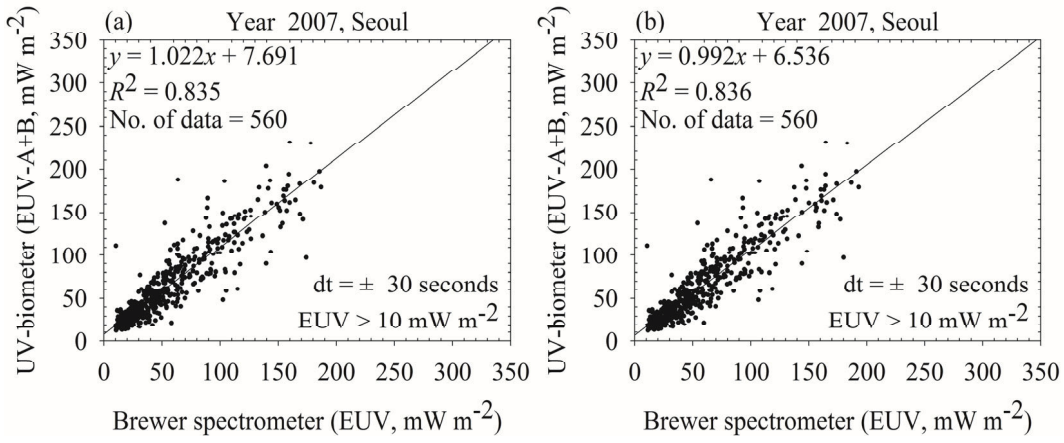

Fig. 7. (a) As in Fig. 6 but for the overlap effect using the ratio of EUV(320/340). (b) As in (a) but for the Brewer spectral UV simulated up to 400 nm.

tween the two instruments' data. Furthermore, the temporal variation of clouds and aerosol types also affects the disagreement.

4. Summary and discussion

From the radiative model simulation, the EUV in the UV-A region affects the 15–31 mW m^{-2} range for EUV, which is 0.6–1.2 for the UV-index. Furthermore, the proportion of EUV(A+B) to EUV(B) ranges from 1.20 to 1.81 in the simulation. Therefore, solely using a UV-biometer for the UV-B region can underestimate the EUV. To deal with the EUV underestimation from the broadband observation, the TUV data in the UV-A region can be utilized to supplement the EUV in the UV-A region. In order that the absorption and scattering properties are spectrally varied, however, the impact of the UV-A region for EUV is impossible to directly estimate from the broadband observation. Therefore, the coefficient of EUV(A)/TUV(A) is introduced by using the simulated spectral irradiance, and it is found that the EUV(A)/TUV(A) is changed by the condition of SZA, total ozone, and AOD due to the spectral change of extinction and optical path length. The EUV(A)/TUV(A) is estimated by the range from 6.1×10^{-4} to 7.0×10^{-4} as the change of the seasonal condition, and the representative value is 6.9×10^{-4}. The relative variance of the EUV(A)/TUV(A) due to total ozone and AOD is 3.9% and 4.4%, respectively.

After testing the sensitivity to the EUV(A)/TUV(A), an LUT for EUV(A)/TUV(A) is developed as a function of SZA, total ozone, and AOD at 550 nm. The methods using a fixed EUV(A)/TUV(A) value of 6.9×10^{-4}, and taking the value from the LUT, are used to estimate the EUV(A) from the broadband observation in the UV-A region. By adopting the EUV(A)/TUV(A) as the observation, the EUV(A+B) is determined from the broadband observation. The estimated EUV(B) and EUV(A+B) from the UV-biometer data are compared with those from the Brewer spectrophotometer at the same site at Yonsei University. By using the observational data from the year 2007, both methods estimate that the EUV(A) takes about 15% of total EUV irradiance, but the difference in EUV(A) between the two methods is insignificant. This is because the difference in EUV(A) between both methods is $2.1\% \pm 2.3\%$. The insignificant difference is due to the small variation of the EUV(A)/TUV(A) in the LUT.

From the statistical analysis for validation, the EUV(B) from solely using the UV-biometer 501 explains only 95% of total EUV from the Brewer spectrophotometer, but the EUV(A+B) from jointly using the UV-biometers and the Brewer spectrophotometer shows an overestimation of 10%. Because the UV-biometer 501 in the UV-B region have spectral sensitivity in the range from 320 to 340 nm, a correction factor for the EUV(320/340) is developed and adopted in the EUV(A+B). Due to the correction of the EUV(320/340), the EUV(A+B) irradiance has an intensity decrease of 8% for the total EUV, and the EUV(A+B) from the broadband observation shows a statistically significant agreement compared to the result from the spectral observation of the Brewer spectrophotometer.

Although the intensity of EUV is coincident by considering EUV(A), the R^2 value is estimated to be 0.818 to 0.836, which shows insignificant changes as a result of the several improvements. Although this study considers the condition of SZA, total ozone, and AOD, additional sensitivity studies of the EUV(A)/TUV(A) for clouds and aerosol types are required. Partial disagreement of the EUV data between the Brewer spectrophotometer and UV-biometers still remains, due to the limitation of the spectral coverage of the Brewer spectrophotometer. Therefore, the effect of the spectral limitation of the Brewer spectrophotometer is another essential avenue of research in the quest for accurate estimations of EUV(A+B) from Brewer spectrophotometer measurements.

Acknowledgements. This work was supported by the Eco Innovation Program of Korea Environmental Industry and Technology Institute (KEITI) (Grant No. 2012000160002), Korea, and the Brain Korea Plus Program.

REFERENCES

Caldwell, M. M., L. O. Björn, J. F. Bornman, S. D. Flint, G. Kulandaivelu, A. H. Teramura, and M. Tevini, 1998: Effects of increased solar ultraviolet radiation on terrestrial ecosystems. *Journal of Photochemistry and Photobiology B: Biology*, **46**, 40–52.

Cho, H. K, B. Y. Lee, J. Lee, and S. Park, 2001: A seasonal climatology of erythemal ultraviolet irradiance over Korea. *Asia-Pac. J. Atmos. Sci.*, **37**, 525–539.

Griggs, M., 1968: Absorption coefficients of ozone in the ultraviolet and visible regions. *The Journal of Chemical Physics*, **49**, 857–859.

Inn, E. C. Y., and Y. Tanaka, 1953: Absorption coefficient of ozone in the ultraviolet and visible regions. *Journal of the Optical Society of America*, **43**, 870–872.

Kim, J., S. S. Park, N. Cho, W. Kim, and H.-K. Cho, 2011: Recent variations of UV irradiance at Seoul 2004 $\sim$ 2010, *Atmosphere*, **21**, 429–438.

Kim, S.-W., S.-C. Yoon, J. Kim, and S.-Y. Kim, 2007: Seasonal and monthly variations of columnar aerosol optical properties over East Asia determined from multi-year MODIS, LIDAR, and AERONET Sun/sky radiometer measurements. *Atmos. Environ.*, **41**, 1634–1651.

Koo, J.-H., 2008: Optical properties of aerosol in a megacity, Seoul from ground-based and satellite measurements. M.S. thesis, Yonsei University, 145 pp.

Koo, J.-H, J. Kim, M. Kim, H.-K. Cho, K. Aoki, and M. Yamano, 2007: Analysis of Aerosol Optical Properties in Seoul using Skyradiometer observation. *Atmosphere*, **17**, 407–420.

Kudish, A. I., V. Lyubansky, E. G. Evseev, and A. Ianetz, 2005: Inter-comparison of the solar UVB, UVA and global radiation clearness and UV indices for Beer Sheva and Neve Zohar (Dead Sea), Israel. *Energy*, **30**, 1623–1641.

Le Quéré, F., and C. Leforestier, 1992: Theoretical calculation of the Huggins band of ozone. *Chem. Phys. Lett.*, **189**, 537–541.

Madronich, S., R. L. McKenzie, L. O. Björn, and M. M. Caldwell, 1998: Changes in biologically active ultraviolet radiation reaching the Earth's surface. *Journal of Photochemistry and Photobiology B: Biology*, **46**, 5–19.

Mayer, B. and A. Kylling, 2005: Technical note: The libRadtran software package for radiative transfer calculations-Description and examples of use. *Atmos. Chem. Phys*, **5**, 1855–1877.

McKinlay, A. F., and B. L. Diffey, 1987: A reference action spectrum for UV induced erythema in human skin. *Human Exposure to Ultraviolet Radiation: Risks and Regulations*, W. F. Passchier and B. F. M. Bosnajakovic, Eds., Elsevier, 83–87.

Molina, L. T., and M. J. Molina, 1986: Absolute absorption cross sections of ozone in the 185-to 350-nm wavelength range. *J. Geophys. Res.*, **91**(D13), 14 501–14 508.

Park, S. S., J. Kim, N. Cho, Y. G. Lee, and H. K. Cho, 2011: The variations of stratospheric ozone over the Korean Peninsula 1985–2009. *Atmosphere*, **21**, 349–359.

Setlow, R. B., 1974: The wavelengths in sunlight effective in producing skin cancer: A theoretical analysis. *Proceedings of the National Academy of Sciences of the United States of America*, **71**, 3363–3366.

Singh, R., S. Nath, R. S. Tanwar, and S. Singh, 2005: Study of erythemal dose variation and exposure time for different UV-B dose levels at Indian mainland and Antarctica. *Proc. URSI*, New Delhi, [Available Online at http://www.ursi.org/Proceedings/ProcGA05/pdf/K04a.9(01460).pdf]

Smith, R. C., Z. M. Wan, and K. S. Baker, 1992: Ozone depletion in Antarctica: Modeling its effect on solar UV irradiance under clear-sky conditions. *J. Geophys. Res.*, **97**(C5), 7383–7397.

Solar Light Co., 1991: *UV-Biometer User's Manual*. Solar Light Co., 459 pp.

Solar Light Co., 2006: *501 UV Biometer Owners Manual*. Solar Light Co., 48 pp.

van Geffen, J., R. van der A, M. van Weele, M. Allart, and H. Eskes, 2004: Surface UV radiation monitoring based on GOME and SCIAMACHY. *Proc. of the 2004 Envisat & ERS Symposium*, Salzburg, Austria.

World Health Organization, 2002: Global Solar UV index. A Practical Guide. World Health Organization, WHO/SDE/OEH/02.2, Geneva, Switcherland, 28 pp.

World Meteorological Organization, 2011: GAW Report No. 198-Data Quality Objectives (DQO) for Solar Ultraviolet Radiation Measurements (Part 1), World Meteorological Organization, 21 pp.